Structural Comparison of Phosphorylated and Unphosphorylated Forms of III^{Glc}, a Signal-Transducing Protein from *Escherichia coli*, Using Three-Dimensional NMR Techniques†

Jeffrey G. Pelton,‡ Dennis A. Torchia,*,‡ Norman D. Meadow,§ and Saul Roseman§

Bone Research Branch, National Institute of Dental Research, National Institutes of Health, Bethesda, Maryland 20892, and Department of Biology and McCollum-Pratt Institute, The Johns Hopkins University, Baltimore, Maryland 21218

Received February 11, 1992

ABSTRACT: The 18.1-kDa protein III^{Glc} from *Escherichia coli* acts as both a phosphocarrier protein in the phosphoenolpyruvate:glycose phosphotransferase system (PTS) and as a signal-transducing protein with respect to the uptake of non-PTS sugars. Phosphorylation of III^{Glc} at the N^{ϵ} (N3) position of His-90 was effected through a regeneration system that included $MgCl_2$, DTT, excess PEP, and catalytic amounts of Enzyme I and HPr. NH, ^{15}N, and $^{13}C\alpha$ signal assignments for P-III^{Glc} were made through comparison of ^{15}N–^{1}H correlation spectra (HSQC) of uniformly ^{15}N-labeled preparations of phosphorylated and unphosphorylated protein and through analysis of three-dimensional triple-resonance HNCA spectra of P-III^{Glc} uniformly labeled with both ^{15}N and ^{13}C. Backbone and side-chain ^{1}H and $^{13}C\beta$ signals were assigned using 3D heteronuclear HCCH-COSY and HCCH-TOCSY spectra of P-III^{Glc}. Using this approach, the assignments were made without reference to nuclear Overhauser effect data or assumptions regarding protein structure. The majority of NH, ^{15}N, Hα, and $^{13}C\alpha$ chemical shifts measured for P-III^{Glc} were identical to those obtained for the unphosphorylated protein [Pelton, J. G., Torchia, D. A., Meadow, N. D., Wong, C.-Y., & Roseman, S. (1991) *Biochemistry 30*, 10043]. Those signals that exhibited shifts corresponded to residues within four segments (1) Leu-87–Gly-100, (2) Val-36–Val-46, (3) His-75–Ser-78, and (4) Ala-131–Val-138. These four segments are in close proximity to the active site residues His-75 and His-90 in the unphosphorylated protein [Worthylake, D., Meadow, N. D., Roseman, S., Liao, D., Hertzberg, O., & Remington, S. J. (1991) *Proc. Natl. Acad. Sci. U.S.A. 88*, 10382], and the chemical shift data provide strong evidence that if any structural changes accompany phosphorylation, they are confined to residues in these four segments. This conclusion is confirmed by comparing NOEs observed in 3D $^{15}N/^{13}C$ NOESY-HMQC spectra of the two forms of the protein. No NOE differences are seen for residues having the same chemical shifts in III^{Glc} and P-III^{Glc}. Furthermore, with the exception of residues Ala-76, Asp-94, and Val-96, the NOEs of residues (in the four segments) which exhibited chemical shift differences also had the same NOEs in III^{Glc} and P-III^{Glc}. In the case of residues Ala-76, Asp-94, and Val-96, minor differences in NOEs, corresponding to interproton distances changes of less than 1.5 Å, were observed. Together, the data show that no large structural rearrangements occur in III^{Glc} upon phosphorylation and that the minor structural changes (<1.5 Å) seen are limited to the active site. Hence, the results of structural studies of III^{Glc} may be appropriate to modeling studies of the interaction of P-III^{Glc} with HPr and other PTS and non-PTS proteins.

The phosphoenolpyruvate:glycose phosphotransferase system (PTS)[1] mediates the transport and concomitant phosphorylation of its sugar substrates and regulates the uptake of other carbon sources in response to changing environmental conditions. Glucose transport and phosphorylation via the PTS occurs in a multistep process whereby a phosphoryl group derived from phosphoenolpyruvate (PEP) is transferred sequentially to the proteins Enzyme I, HPr, and III^{Glc}. Subsequently, a complex between phospho-III^{Glc} (P-III^{Glc}) and the membrane-associated protein IIB^{Glc} acts to phosphorylate and transport a glucose molecule into the cell.

As part of its role as a phosphocarrier protein, *Escherichia coli* III^{Glc} (18.1 kDa, 168 amino acids) is phosphorylated at the N^{ϵ} (N3) position of His-90 by HPr (Meadow & Roseman, 1982; Dörschug et al., 1984). Replacement of His-90 with glutamine by site-directed mutagenesis results in the complete loss of activity. In contrast, replacement of His-75 with glutamine results in loss of phosphodonor but not phosphoacceptor activity, indicating that both histidine residues are important for normal function (Presper et al., 1989). It was recently shown that His-75 and His-90 are close in space (Pelton et al., 1991b; Worthylake et al., 1991).

† This work was supported by the AIDS Targeted Antiviral Program of the Office of the Director of the National Institutes of Health (to D.A.T.) and Grant GM 38759 from the National Institutes of Health and Grant N00014-91-J-4033 from the Office of Naval Research (to S.R.).

* Author to whom correspondence should be addressed.

‡ NIH.

§ The Johns Hopkins University.

[1] Abbreviations: COSY, correlation spectroscopy; crr, catabolite repression resistance; DANTE, delays alternating with nutation for tailored excitation; DTT, dithiothreitol; HCCH-COSY, 3D ^{1}H–^{13}C–^{13}C–^{1}H correlation via J_{CC} couplings; HCCH-TOCSY, 3D ^{1}H–^{13}C–^{13}C–^{1}H total correlation spectroscopy via isotropic mixing of ^{13}C magnetization; HMQC, heteronuclear multiple-quantum spectroscopy; HNCA, amide proton to nitrogen to α-carbon correlation; HOHAHA, homonuclear Hartmann–Hahn spectroscopy; HSQC, heteronuclear single-quantum spectroscopy; NMR, nuclear magnetic resonance; NOE, nuclear Overhauser effect; NOESY, nuclear Overhauser effect spectroscopy; PEP, phosphoenolpyruvate; TOCSY, total correlation spectroscopy; 1D, one dimensional; 2D, two dimensional; 3D, three dimensional; $III^{Glc}N$, uniformly ^{15}N-labeled III^{Glc}_{slow}; $III^{Glc}NC$, uniformly $^{15}N/^{13}C$-labeled III^{Glc}_{slow}.

0006-2960/92/0431-5215$03.00/0

The N-terminal peptide of III^{Glc} is also required for phosphodonor activity. During purification, two forms of III^{Glc} are isolated that have different electrophoretic mobilities on polyacrylamide gels (Meadow & Roseman, 1982). The faster migrating form, denoted III^{Glc}_{fast}, is derived from the slower migrating form (III^{Glc}_{slow}) through cleavage of the first seven residues by a membrane-associated endopeptidase (Meadow et al., 1986). III^{Glc}_{fast} retains its phosphoacceptor activity but has lost most of its phosphodonor activity (Meadow & Roseman, 1982).

Regulation via the PTS involves transduction of signals from the environment to the genome, resulting in enhanced or repressed expression of genes needed to catabolize non-PTS sugars. The *crr* gene, which is required for this regulatory function, was shown to encode III^{Glc}. As a signal-transducing protein, III^{Glc} has been shown to bind to and inhibit several non-PTS permeases including those for lactose, melibose, maltose, and also glycerol kinase. In contrast, the phosphorylated form of III^{Glc} does not inhibit these permeases and may stimulate adenylate cyclase. The molecular basis for the latter regulatory phenomenon is unknown. [For recent reviews, see Meadow et al. (1990), Roseman and Meadow (1990), Saier (1989), and Postma and Lengeler (1985).]

Early structural studies of PTS proteins include 1D NMR investigations of HPr (Kalbitzer et al., 1982, 1985), factor III from the lactose PTS (III^{Lac}) (Kalbitzer et al., 1981), and III^{Glc} (Dörschug et al., 1984). The tertiary structure of HPr determined using 2D NMR methods (Hammen et al., 1991; Klevit & Waygood, 1986) was not in agreement with an X-ray crystallographic determination (El-Kabbani et al., 1987) and is an area of active research (Wittekind et al., 1990; Kapadia et al., 1990; Hammen et al., 1991).

We have reported virtually complete ^1H, ^{15}N, and ^{13}C NMR signal assignments (Pelton et al., 1991a) and have elucidated many elements of secondary structure (Pelton et al., 1991b) for III^{Glc}_{slow} from *E. coli* using double- and triple-resonance 3D NMR techniques (Ikura et al., 1990a, 1991; Kay et al., 1990a). Recently, a model for the tertiary structure of III^{Glc}_{fast} was proposed on the basis of X-ray data obtained at 2.1-Å resolution (Worthylake et al., 1991). The secondary structure in solution deduced using NMR methods was consistent with that obtained in the crystalline state using X-ray methods (Worthylake et al., 1991).

Heteronuclear 3D NMR (Fairbrother et al., 1991) and X-ray studies (Liao et al., 1991) have also been reported for the IIA^{Glc} domain of the *Bacillus subtilis* glucose permease. This protein has 42% sequence identity with *E. coli* III^{Glc} and complements a *crr* mutation in *E. coli* (Gonzy-Treboul & Steinmetz, 1987). Although structures of the active sites of the *E. coli* and *B. subtilis* proteins are the same, structural differences do exist (Worthylake et al., 1991).

Analysis of X-ray data obtained for a chloroplatinate heavy atom derivative of *E. coli* III^{Glc} in which the metal coordinates N^{ϵ} atoms of His-75 and His-90, in conjunction with model building, led to the hypothesis that no significant structural changes would occur in the protein upon phosphorylation (Worthylake et al., 1991). The same hypothesis was advanced regarding the structure of the phosphorylated *B. subtilis* IIA^{Glc} domain (Liao et al., 1991). In order to better understand the role of phospho-III^{Glc} both as a phosphocarrier protein and as a regulatory protein, and to test the hypothetical structural models for P-III^{Glc} advanced on the basis of crystallographic data of the unphosphorylated proteins, we have assigned the majority of ^1H, ^{15}N, $^{13}C\alpha$, and $^{13}C\beta$ signals of phospho-III^{Glc} from *E. coli* using 3D double- and triple-resonance NMR techniques and have compared the structures of the phosphorylated and unphosphorylated forms of the protein using extensive chemical shift and NOESY data.

Materials and Methods.

III^{Glc}_{slow} was overexpressed using *E. coli* strain BL21 (DE3) (Studier & Moffatt, 1986) that was transformed with the gene for III^{Glc} (*crr* gene) under control of the T7 promoter (a gift from Dr. V. Chaudhary, National Institutes of Health). Cells were grown as described (Pelton et al., 1991a; Meadow & Roseman, 1982) on the minimal medium of Neidhart et al. (1974) with 0.2% glucose and supplemented with 2 mg/mL thiamine and 50 mg/mL ampicillin. Uniformly ^{15}N- and $^{15}N/^{13}C$-labeled samples were obtained by growing cells on either $^{15}NH_4Cl$ or $^{15}NH_4Cl/[^{13}C_6]$glucose as the sole nitrogen and sole nitrogen/carbon sources, respectively. The ^{15}N- and $^{15}N/^{13}C$-labeled protein samples will hereafter be denoted $III^{Glc}N$ and $III^{Glc}NC$. The purity of each sample was greater than 97% based on SDS–PAGE followed by quantitative densitometric scanning of the Coomassie-stained gel. Enzyme I and HPr were obtained from *Salmonella typhimurium* as described (Wiegel et al., 1982; Beveshi et al., 1982).

A regeneration system was used to keep III^{Glc} phosphorylated during each experiment (Waygood et al., 1979). To 16 mg of III^{Glc}_{slow} dissolved in 450 μL of a solution containing 0.15 M KCl and 1 mM $MgCl_2$ (pH 6.4), catalytic amounts of HPr (1.6 μM) and Enzyme I (5 units) were added along with excess phosphoenolpyruvate [potassium 2-(phosphonooxy)-2-propenoate] (pH 6.4) (Sigma, St. Louis, MO.). For experiments that required less than 1 day to record, a phosphoenolpyruvate concentration of 3.8–5 mM was used. For longer experiments (up to 3 days), higher phosphoenolpyruvate concentrations were needed (50–100 mM). In addition, for longer experiments dithiothreitol (DTT) (1 mM) was added to stabilize Enzyme I, and potassium phosphate (30 mM, pH 6.4) was added to control pH. No chemical shift changes were observed in ^{15}N HMQC spectra of $III^{Glc}N$ upon addition of DTT, potassium phosphate, or high concentrations (up to 100 mM) of phosphoenolpyruvate. From these observations, it was concluded that these compounds did not induce structural changes in $III^{Glc}N$ at the stated concentrations. For samples dissolved in H_2O, the extent of phosphorylation was checked at the beginning and at the end of each experiment by noting the change in intensity of the NH signal of Lys-132 (9.83 ppm P-$III^{Glc}N$; 9.76 ppm $III^{Glc}N$ at pH 6.4 and 308 K) in ^{15}N-filtered 1D spectra of III^{Glc}. Typically, 30 min was required for the complete conversion (>95%) of III^{Glc} into P-III^{Glc}.

For experiments acquired in D_2O, amide protons were exchanged for deuterions by heating the protein sample for approximately 6 h at 60 °C, after which the sample was repeatedly lyophilized and finally redissolved in 450 μL of D_2O (99.998%, Cambridge Isotopes, Woburn, MA). Phosphoenolpyruvate was dissolved in H_2O, and the pH was adjusted with small aliquots of concentrated HCl or KOH to 6.4. DTT (1 mM) and a catalytic amount of HPr were added (1.6 μM) to the PEP solution. This preparation was lyophilized, dissolved in D_2O, and added to the protein sample. Enzyme I (2.3 mg/mL in H_2O) was diluted 10-fold with D_2O and an aliquot (5 units) was added 1 h prior to the beginning of each experiment to initiate the phosphorylation reaction. The degree of phosphorylation was checked at the end of each experiment recorded in D_2O by adding 100 μL of H_2O and allowing 30 min for exchange of labile amide protons. As for experiments conducted in H_2O, the NH signal of Lys-132 proved to be a convenient marker because of its short half-life for exchange (<7 min at pH 6.4).

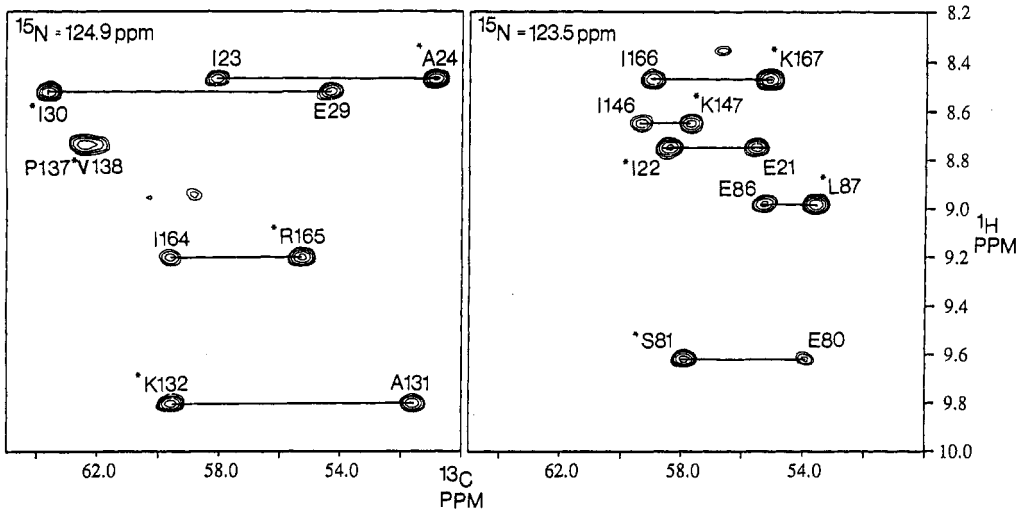

FIGURE 1: Representative planes of a HNCA spectrum of P-III^{Glc}NC at ^{15}N chemical shifts of 124.9 ppm (A) and 123.5 ppm (B). Intraresidue $^{1}H_i$–$^{15}N_i$–$^{13}C\alpha_i$ correlations, denoted by asterisks, are connected by lines with interresidue $^{1}H_i$–$^{15}N_i$–$^{13}C\alpha_{i-1}$ correlations. Labels denote $^{13}C\alpha$ signal assignments. The sample was prepared as follows: 2.0 mM III^{Glc}, 0.15 M KCl, 1 mM $MgCl_2$, 1 μM HPr, 5 units of Enzyme I, 100 mM PEP, 1 mM DTT, and 30 mM phosphate buffer at pH 6.4.

NMR Spectroscopy. All NMR spectra were recorded at pH 6.4 and at 36.5 °C on an AM-500 spectrometer modified to reduce overhead time at the end of each (t_1,t_2) increment (Kay et al., 1990a). The only exception was the 3D ^{15}N TOCSY-HMQC spectrum (see below), which was recorded at pH 7.5. This spectrum was acquired during the initial stages of the work when solvent conditions were still being optimized. For spectra acquired in H_2O, a DANTE pulse train (Kay et al., 1989) of ca. 25 Hz was used to suppress the solvent resonance. The residual solvent signal was subtracted from each free induction decay prior to Fourier transformation using the method of Marion et al. (1989a). For spectra acquired in D_2O, no presaturation was used.

2D ^{15}N HSQC spectra of P-III^{Glc}N were recorded and processed as described (Pelton et al., 1991a) using the Overbodenhausen pulse sequence (Bax et al., 1990a). 3D ^{15}N NOESY-HMQC (Marion et al., 1989b; Kay et al., 1989) and 3D ^{15}N TOCSY-HMQC spectra (Marion et al., 1989c) of P-III^{Glc}N, and 3D ^{13}C NOESY-HMQC (Ikura et al., 1990b) and triple-resonance HNCA spectra (Ikura et al., 1990a, 1991; Kay et al., 1990a) of P-III^{Glc}NC, were also recorded as described (Pelton et al., 1991a). For the 3D ^{15}N NOESY-HMQC experiment, the mixing time was set to 100 ms. For the 3D ^{15}N TOCSY-HMQC experiment, the spectrum was acquired at pH 7.5 with the mixing time set to 36 ms using a DIPSI-2 pulse train (Shaka et al., 1988). For the HNCA experiment, the mixing time during which ^{15}N and $^{13}C\alpha$ signals become antiphase was set to 22 ms. The 3D ^{15}N NOESY-HMQC and ^{15}N TOCSY-HMQC spectra were obtained using 64 scans per complex (t_1,t_2) point. HNCA spectra were acquired with 128 scans per complex (t_1,t_2) increment using a 32-step phase cycle. 3D HCCH-COSY and HCCH-TOCSY spectra of P-III^{Glc}NC were recorded in D_2O using published parameters (Kay et al., 1990b; Bax et al., 1990b,c; Clore et al., 1990). For the HCCH-COSY spectrum, 64 scans per complex (t_1,t_2) point were recorded with a 16-step phase cycle. For the HCCH-TOCSY spectrum, 128 scans per complex (t_1,t_2) point were recorded with a 32-step phase cycle and a mixing time of 24 ms.

Commercial (NMRi, Syracuse, NY) and inhouse software (Garrett et al., 1991; Kay et al., 1989) were used to process the various 2D and 3D spectra. Chemical shifts were referenced to H_2O (4.67 ppm, 36.5 °C), external liquid ammonia (^{15}N), and sodium 3-[2,2,3,3-$^{2}H_4$]trimethylsilylpropionate (TSP) (^{13}C) (Live et al., 1984). Uncertainties in chemical shifts were 0.02 and 0.1 ppm for ^{1}H and heteronuclei, respectively.

Results

^{1}H, ^{15}N, and ^{13}C Signal Assignments. ^{15}N HSQC spectra of III^{Glc}N (2.0 mM) dissolved in a solution containing 0.15 M KCl, 3.8 mM phosphoenolpyruvate (PEP), 1 mM $MgCl_2$, and 1 μM HPr (pH 6.4) were identical to spectra recorded previously (Pelton et al., 1991a) with a sample of III^{Glc}N dissolved in 0.15 M KCl (pH 6.4). Upon addition of 5 units of Enzyme I (16 nM), pronounced changes occurred in the spectrum, presumably due to phosphorylation of III^{Glc}. This result was confirmed by obtaining a ^{15}N HSQC spectrum of a sample which was shown to be 10% phosphorylated by polyacrylamide gel electrophoresis. As expected, the spectrum contained signals associated with III^{Glc}N and weak signals at chemical shifts identical to those obtained with III^{Glc}N dissolved in buffer containing KCl, PEP, $MgCl_2$, HPr, and Enzyme I.

A total of 161 out of a possible 171 ^{15}N–^{1}H correlations were identified in the ^{15}N HSQC spectrum of P-III^{Glc}N, taking into account that III^{Glc} contains seven proline, four asparagine, and one glutamine residue (Supplementary Material). Tentative sequential assignments for approximately 80% of the ^{15}N–^{1}H signals of P-III^{Glc} were obtained through comparison with a ^{15}N HSQC spectrum of the unphosphorylated protein. Information needed to confirm and extend the assignments was obtained from a 3D HNCA spectrum (Ikura et al., 1990a; Kay et al., 1990a) of P-III^{Glc}NC (Figure 1). In this experiment, each ^{15}N–^{1}H correlation is linked to its own $^{13}C\alpha$ signal, and in many cases to the $^{13}C\alpha$ signal of the preceding residue. Because the one-bond $^{13}C\alpha$–^{15}N coupling constant (~11 Hz) is generally larger than the two-bond $^{13}C\alpha$–^{15}N coupling constant (~7 Hz), in most cases intraresidue correlations are more intense and can be distinguished from less intense interresidue correlations. A total of 139 out of a possible 161 $^{13}C\alpha$ assignments were obtained from this 3D spectrum. These data were used in conjunction with interresidue $^{1}H_i$–$^{15}N_i$–$^{13}C\alpha_{i-1}$ correlations to confirm the initial NH assignments and sequentially assign the remaining ^{15}N–^{1}H signals. The assignment process was also aided by comparison of $^{13}C\alpha$ signals with those obtained previously for III^{Glc} (Pelton et al., 1991a). The observed linkages are summarized in

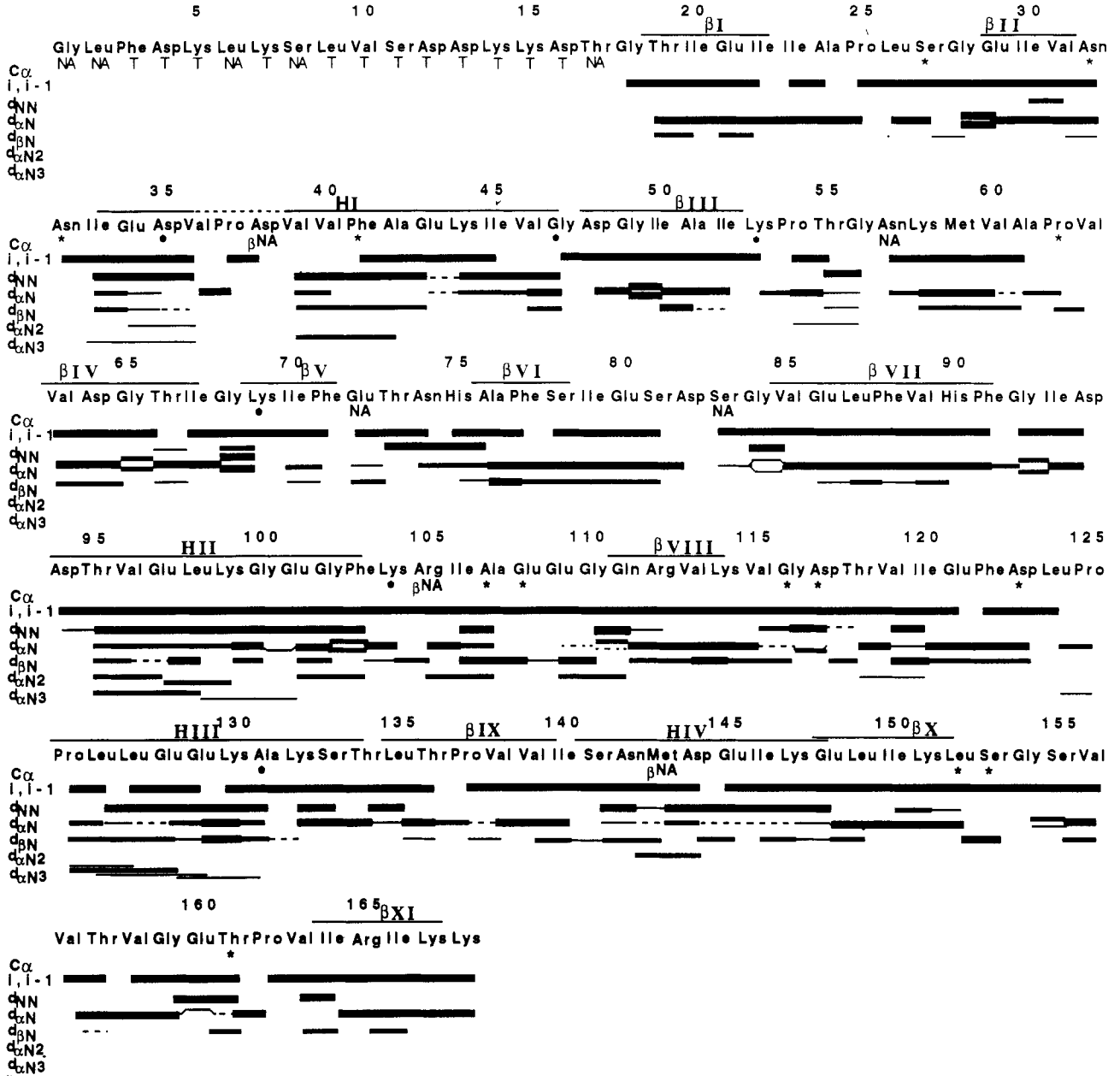

FIGURE 2: Summary of sequential and medium-range NOEs observed in a 3D ^{15}N NOESY-HMQC spectrum of P-III^{Glc}N acquired with a mixing time of 100 ms, and summary of sequential $^{13}C\alpha_{i,i-1}$ linkages obtained from an HNCA spectrum of P-III^{Glc}NC. Medium-range $d_{\alpha N}(i,i+2)$ and $d_{\alpha N}(i,i+3)$ NOEs are denoted $d_{\alpha N}2$ and $d_{\alpha N}3$, respectively. Proline $d_{\alpha\delta}(i,i+1)$ and/or $d_{N\delta}(i,i+1)$ NOEs observed in 3D ^{13}C and ^{15}N NOESY-HMQC spectra are indicated as $d_{\alpha N}$ connectivities. Cross peaks were classified as strong, medium, or weak; line thickness is used to represent cross-peak intensity. Dashed lines indicate overlap of two or more resonances. H and β denote those residues in helical regions and β-strands, respectively. The helical regions may be slightly shorter than represented due to ambiguities in differentiation of helical termini and turns. Asterisks under amino acid labels denote CαH protons that resonate near H_2O (4.67 ± 0.05 ppm) and, as a consequence, were at least partially saturated by the off-resonance DANTE presaturation pulse. The letter T denotes the tentative sequential assignment of a ^{15}N–^{1}H correlation based on comparison of ^{15}N HSQC spectra of phosphorylated and unphosphorylated forms of III^{Glc}; NA and βNA, amide NH or CβH protons, respectively, were not assigned. Note that Asn-32, Val-63, Pro-125, and Val-156 have been repeated on each side of the figure.

Figure 2. Note that breaks occur at each of the seven proline residues because they lack amide protons and are therefore not observable in HNCA spectra.

Several ^{15}N–^{1}H signals tentatively assigned to residues within the 18 amino acid N-terminus were particularly weak in ^{15}N HSQC spectra of P-III^{Glc}. Moreover, no correlations were observed for Gly-1, Leu-2, Leu-6, Ser-8, or Thr-17 accounting for five of the ten missing ^{15}N–^{1}H signals. For unphosphorylated III$^{Glc}_{slow}$, it was found that the first 18 residues were flexible in solution (Pelton et al., 1991b), and the corresponding residues in III$^{Glc}_{fast}$ were not observed in an X-ray analysis (Worthylake et al., 1991). For the first 18 residues of P-III^{Glc}, no correlations were observed in either HNCA or 3D ^{15}N NOESY-HMQC spectra (see below), and therefore the ^{15}N–^{1}H assignments for these residues remain tentative. In addition, those side-chain ^{1}H signals corresponding to the first 18 residues that were identified in HCCH-COSY and HCCH-TOCSY spectra of P-III^{Glc}NC produced particularly strong cross peaks and occurred at similar chemical shifts as those observed in spectra of the unphosphorylated protein. Taken together, these data indicate that the first 18 amino acids of P-III^{Glc} behave like those of III^{Glc} (Pelton et al., 1991b) in that they are flexible in solution and do not interact significantly with the rest of the molecule.

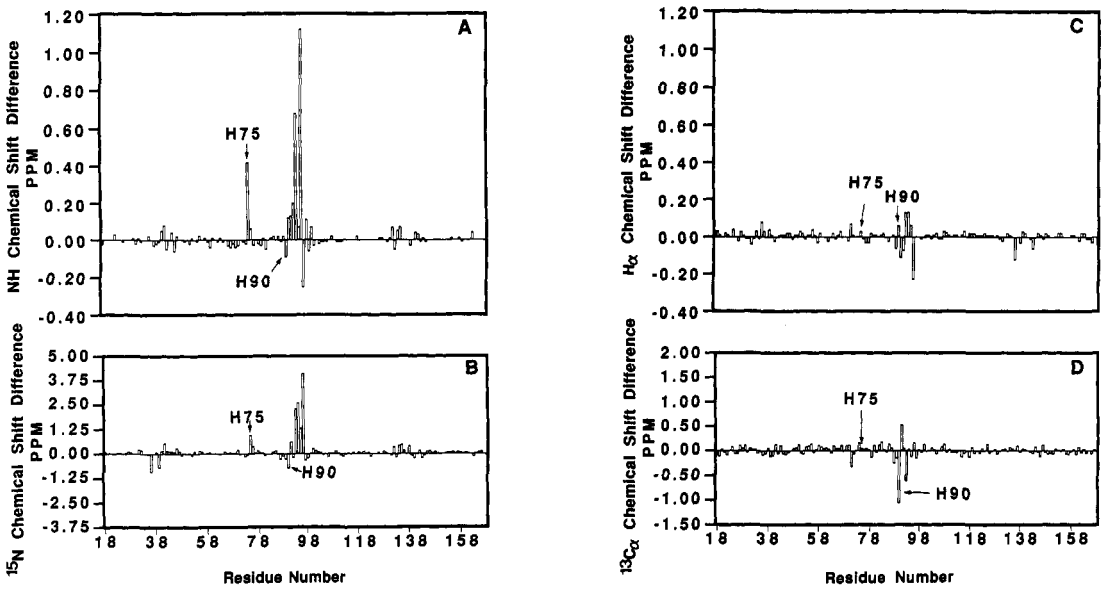

FIGURE 3: Chemical shift differences for NH (A), ^{15}N (B), Hα (C), and ^{13}Cα (D) signals of the structured residues (residues 18–168) of P-III^{Glc} that result from phosphorylation of His-90. Chemical shift differences of all nuclei are normalized with respect to Hertz. Residues His-75 and His-90 are denoted with labels. In addition to the seven proline residues which lack NH protons, ^{15}N–^{1}H signals for Asn-57, Glu-72, and Ser-83 were not determined. The chemical shift differences for these residues were therefore set to zero.

In addition to the five signals not observed in the N-terminus of ^{15}N HSQC spectra of P-III^{Glc}N, NH signals were not identified for Asn-57, Glu-72, or Ser-83. NH signals for Asn-57 and Ser-83 were also not identified in our study of III^{Glc} (Pelton et al., 1991a). The two remaining NH correlations are accounted for by the degeneracy of ^{15}N–^{1}H chemical shifts for the pairs of residues F91–R105 and G65–G18.

Initial assignments of side-chain signals of P-III^{Glc} were obtained from a 3D ^{15}N TOCSY-HMQC spectrum acquired at pH 7.5. From this experiment, approximately 63% of the Hα signals, in addition to many Hβ and other side-chain resonances, were correlated with their own ^{15}N–^{1}H signals. These data along with ^{13}Cα chemical shifts obtained from the HNCA spectrum of P-III^{Glc}NC were used to assign the majority of side-chain ^{1}H and ^{13}Cβ resonances through analysis of HCCH-COSY and HCCH-TOCSY spectra of P-III^{Glc}NC as described (Pelton et al., 1991a) (Supplementary Material).

Chemical Shift Differences. The chemical shift of a nucleus (^{15}N, ^{13}C, or ^{1}H) is dependent on a number of important factors (Spera & Bax, 1991; Wishart et al., 1991; Witanowski et al., 1986; Howarth & Lilley, 1978), and it is well known that chemical shift differences reflect changes in conformation and/or the local environment of a spin (Wittekind et al., 1989). NH and ^{15}N chemical shift differences that occur due to phosphorylation are shown in relation to the sequence of III^{Glc} in Figure 3A,B. Comparison can also be made of ^{1}H and ^{13}C signals if it is assumed, as was the case for ^{15}N and NH resonances, that the observed shift differences are the result of phosphorylation and are not due to the addition of HPr, $MgCl_2$, DTT, and PEP (Figure 3C,D). As can be seen from these data, the majority of NH, ^{15}N, Hα, and ^{13}Cα signals do not change significantly upon phosphorylation. Moreover, those signals that do change are clustered into four segments. Some of the largest changes are associated with residues in the segment Leu-87–Gly-100, while smaller changes are observed for residues in the segments Val-36–Val-46, His-75–Ser-78, and Ala-131–Val-138. Fewer changes were noted for Hβ and ^{13}Cβ signals. These include residues Ala-76 (Hβ change in chemical shift relative to III^{Glc}, −0.11 ppm; ^{13}Cβ, −1.0 ppm), Val-96 (Hβ, 0.23 ppm; ^{13}Cβ, −0.8 ppm), Thr-95

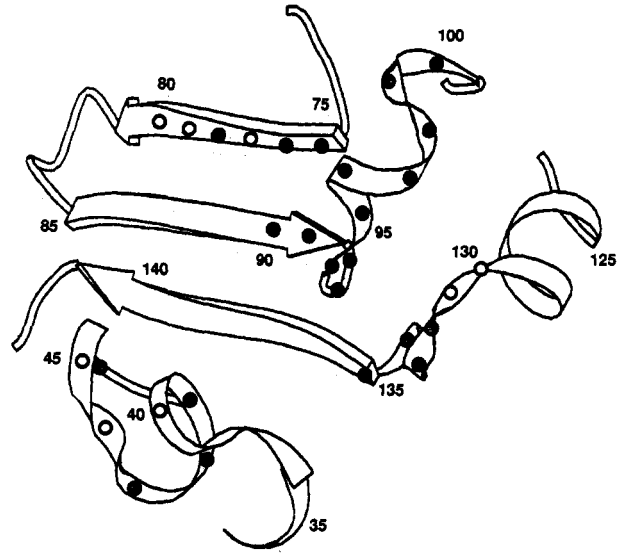

FIGURE 4: Ribbon diagram of a portion of the X-ray structure of unphosphorylated III^{Glc} including active site residues His-75, His-90, and those residues whose NH signals show significant shifts. Circles denote residue positions within the structure. NH signals that show large chemical shift differences as a result of phosphorylation (≥0.10 ppm) are denoted with black circles, while those that shift an intermediate amount (±0.05 to ±0.10 ppm) are denoted with hatched circles. For clarity, open circles are used to denote the positions of some residues for which the corresponding NH signal did not change. This figure is based on the X-ray structure of unphosphorylated III^{Glc} (Worthylake et al., 1991) and was created with the Molscript software graphics package (Kraulis, 1991).

Hβ (+0.14 ppm), and Phe-91 ^{13}Cβ (−0.4 ppm). Chemical shift differences for the remaining aliphatic side-chain protons that were identified in HCCH-COSY and HCCH-TOCSY spectra of P-III^{Glc} differed by less than ±0.10 ppm from those reported previously (Pelton et al., 1991a). A portion of the X-ray structure of the unphosphorylated form of III^{Glc} (Worthylake et al., 1991) that includes these four segments is shown in Figure 4. From these data, it can be seen that all of the signals that shift upon phosphorylation are associated with residues that are close to His-90, the site of phosphorylation.

3D ^{15}N and ^{13}C NOESY-HMQC Spectra. Detailed infor-

mation about the structure of a protein can be deduced from short-range (<5 Å) internuclear ^1H–^1H distances (NOEs) obtained from 3D ^{15}N and ^{13}C NOESY-HMQC spectra (Wüthrich, 1986; Bax, 1989; Clore & Gronenborn, 1991). The intensity of a NOE cross peak is a function of the inverse sixth power of the distance between the spins (Kalk & Berendsen, 1976) and is therefore sensitive to relatively small distance changes. For example, a reduction in the intensity of a NOE cross peak by a factor of 10 corresponds to an increase in the distance between a pair of spins initially 2.4 Å apart to 3.5 Å, neglecting spin diffusion effects. NOE cross peaks for active site residues His-75 and His-90, as well as for those residues whose NH signals shift by ±0.09 ppm or more upon phosphorylation, are shown in Figure 5A,B along with NOE cross peaks obtained for these residues in the unphosphorylated state. It should be noted that use of a regeneration system to keep III^{Glc} phosphorylated necessitated acquiring 3D ^{15}N and ^{13}C NOESY-HMQC spectra of P-III^{Glc} under different solvent conditions (up to 50 mM PEP, 30 mM potassium phosphate) than those used in our original study of III^{Glc}. As stated previously, the change of conditions did not result in structural changes to the protein as measured by ^{15}N–^1H chemical shifts. However, the use of high concentrations of PEP resulted in t_1 noise and a reduction in the signal to noise ratio for the ^{15}N NOESY-HMQC spectrum of P-III^{Glc} compared to similar spectra of III^{Glc}. As can be seen in Figure 5A,B, chemical shift changes are observed not only for NH signals (diagonal peaks) but also for many side-chain protons that give rise to NOE cross peaks. Because of the chemical shift changes, the peak *positions* in the NOE patterns are not identical. However, since ^1H chemical shift assignments are known for both the phosphorylated and unphosphorylated forms of III^{Glc}, cross peaks in the two spectra can be correlated as shown in Figure 5A,B. Comparison of NOE cross peaks for residues His-75 and His-90 revealed no new NOEs. Moreover, the *relative intensities* of the cross peaks, which relate to internuclear ^1H–^1H distances, are virtually the same in spectra of III^{Glc} and P-III^{Glc} (Figure 5A). One minor exception is the appearance of a weak NOE between His-75 NH and A76 Hβ in spectra of III^{Glc} that is very weak in spectra of P-III^{Glc}. There is also a close correspondence in NOE intensities for residues Gly-92, Ile-93, and Leu-98 in spectra of III^{Glc} and P-III^{Glc} (Figure 5A,B). No new NOEs are observed, and the relative intensities of the cross peaks are the same. Thus, although these residues exhibit different chemical shifts in spectra of III^{Glc} and P-III^{Glc}, there are no significant changes in the internuclear distances between backbone NH protons and neighboring protons.

A comparison of NOE cross peaks for the other ^{15}N–^1H signals that shift by ±0.09 ppm or more (Figure 5) revealed a number of changes (Table I). Several apparent differences in the cross peak patterns for Phe-91 and Glu-97 are due to partial overlap of these ^{15}N–^1H correlations with Arg-105 and Val-36 signals in spectra of P-III^{Glc} but not in spectra of III^{Glc}. Small NOE cross peak intensity changes were also observed for a number of NOEs to the backbone and side-chain protons of Ala-76 and the Hγ protons of Val-96 (Figure 5, Table I); however, the most dramatic differences were observed for Asp-94 (Figure 5, Table I). For this residue, new NOE cross peaks appear at 4.66 and 4.78 ppm in spectra of P-III^{Glc}. The signal at 4.78 ppm corresponds to the Hα signal of Asp-94. In spectra of unphosphorylated III^{Glc}, Asp-94 Hα resonates under the solvent signal at 4.66 ppm and as a consequence was not observed due to saturation along with the solvent by the DANTE pulse train. The signal at 4.66 ppm is coincident with the HDO signal. This peak was not observed in 3D ^{15}N NOESY-HMQC spectra of the unphosphorylated form of III^{Glc} and could not be assigned to any protons near the NH proton of Asp-94. In addition to these new cross peaks, a number of NOEs to Asp-94 NH changed as a result of phosphorylation (Table I). In particular, the relative intensity of the cross peak between NH protons of Asp-94 and Thr-95 is weaker and the relative intensity of the cross peak between Asp-94 NH and His-90 CH^ϵ is stronger in the spectrum of the phosphorylated protein. Furthermore, in the spectrum of unphosphorylated III^{Glc} a weak NOE appears between Asp-94 NH and one of its two Hβ protons at 2.86 ppm (Asp-94 Hβ protons of III^{Glc}, 2.86 and 3.22 ppm), while in the spectrum of the phosphorylated protein an NOE is observed between Asp-94 NH and the other Hβ proton at 3.21 ppm (Asp-94 Hβ or P-III^{Glc}, 2.82 and 3.21 ppm), assuming that the chemical shifts of the Hβ protons are not adventitiously inverted upon phosphorylation.

Table I: NOE Intensity Changes in Spectra of P-III^{Glc} vs III^{Glc}

residues	NOE intensity P-III^{Glc}	NOE intensity III^{Glc}
Ala-76 Hβ–His-75 NH	very weak	weak
Ala-76 Hα–Phe-91 NH	very weak	weak
Ala-76 NH–Ala-76 Hα	weak	medium
Asp-94 NH–(4.66 ppm)[a]	medium	missing
Asp-94 NH–Asp-94 Hα	medium	missing[b]
Asp-94 NH–Thr-95 NH	weak	medium
Asp-94 NH–His-90 CH^ϵ	medium	very weak
Asp-94 NH–Asp94 Hβ1[c]	missing	weak
Asp-94 NH–Asp-94 Hβ2[c]	weak	missing
Asp-94 NH–Ile-93 Hδ	missing	weak
Val-96 NH–Val-96 Hγ1[d]	weak	medium
Val-96 Hγ1–Glu-97 NH[d]	missing	medium

[a] New/unassigned. [b] Asp-94 Hα (4.65 ppm III^{Glc}; 4.78 ppm P-III^{Glc}) resonates under the solvent signal in spectra of III^{Glc} and was saturated by the DANTE pulse train. [c] Hβ1 and Hβ2 refer, respectively, to the upfield (2.86, III^{Glc}; 2.82, P-III^{Glc}) and downfield (3.22 ppm, III^{Glc}; 3.21 ppm P-III^{Glc}) protons of Asp-94, assuming that the frequencies do not invert upon phosphorylation. The labels Hβ1 and Hβ2 are not meant to indicate stereospecific assignment of these protons. [d] Hγ2 and Hγ1 refer, respectively, to the upfield (0.94 ppm, III^{Glc}; 1.00 ppm P-III^{Glc}) and downfield (1.13 ppm III^{Glc}; 1.10 ppm P-III^{Glc}) Hγ protons of Val-96. The labels Hγ2 and Hγ1 are not meant to indicate stereospecific assignment of these protons.

Sequential and medium-range NOEs obtained from a 3D ^{15}N NOESY-HMQC spectrum of P-III^{Glc}N are summarized in Figure 2. As expected based on the similarity of chemical shifts for the two proteins (Figure 3), the overall NOE pattern is essentially the same as observed for unphosphorylated III^{Glc}. Strong $d_{\alpha N}$ NOEs which are characteristic for residues that adopt an extended conformation are observed for each of 11 segments that were previously shown to form portions of antiparallel β-sheet (Pelton et al., 1991b; Worthylake et al., 1991). These segments are numbered βI–βXI in Figure 2. Four segments of strong d_{NN} NOEs (labeled HI–HIV), which are characteristic for residues that adopt helical or turn structures, were also observed and are similar to those seen in spectra of unphosphorylated III^{Glc} (Pelton et al., 1991b). Although the overall NOE patterns were the same, some differences were noted. For example, several weak NOEs were missing in spectra of P-III^{Glc} as a consequence of the lower signal to noise ratio obtained for this spectrum. In addition, as stated above, a significant difference was the reduced intensity of the NOE between NH protons of Asp-94 and Thr-95 (d_{NN} NOE).

As a further comparison of the structures of III^{Glc} and P-III^{Glc}, long-range $d_{\alpha N}(i,j)$, $d_{NN}(i,j)$, and $d_{\alpha\alpha}(i,j)$ NOEs (Wüthrich et al., 1986), where i and j represent residues more

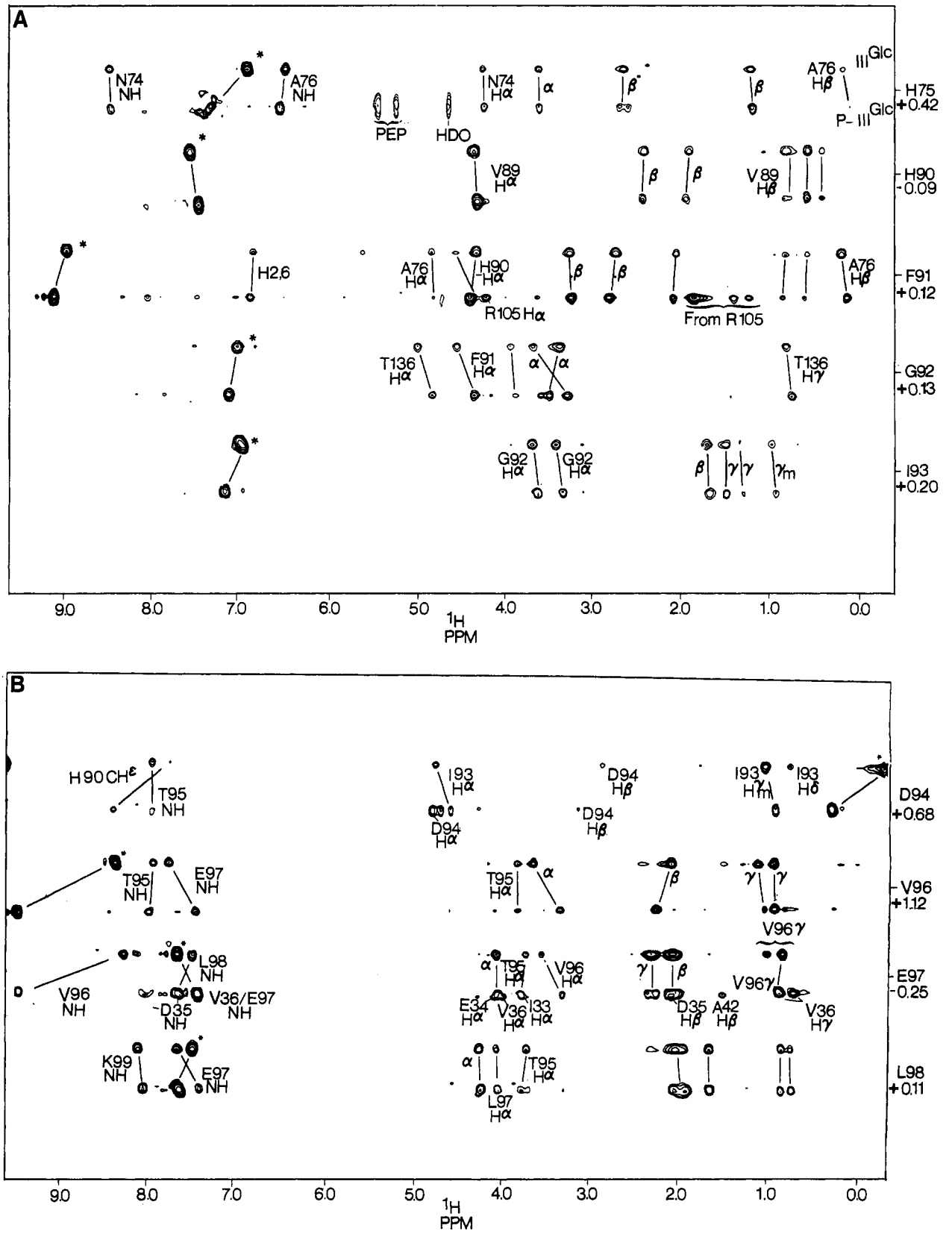

FIGURE 5: Strips taken from 3D ^{15}N NOESY-HMQC spectra of III^{Glc} (top slice) and P-III^{Glc} (bottom slice) for residues whose NH signals shift by ±0.09 ppm or more. NH chemical shift differences referred to unphosphorylated III^{Glc} (ppm) are denoted under the residue labels. Asterisks denote diagonal peaks. Intraresidue NOEs are indicated with greek symbols but no residue labels. Lines correlate NOE cross peaks between identical proton pairs. Note that the diagonal signal of Asp-94 in spectra of both III^{Glc} and P-III^{Glc} is folded. As a consequence it appears on the right rather than on the left edge of the figure. NOE patterns for Phe-91 and Glu-97 are complicated by overlap of ^{15}N–^{1}H signals of Arg-105 and Val-36, respectively, in spectra of P-III^{Glc} but not in spectra of III^{Glc}.

than five residues apart in the primary sequence, were identified in 3D ^{15}N and ^{13}C NOESY-HMQC spectra of P-III^{Glc}N and P-III^{Glc}NC, respectively. These data are summarized in Figure 6 along with the secondary structure of P-III^{Glc}. As can be seen through comparison this figure with that reported previously (Pelton et al., 1991b), nearly all of the long-range

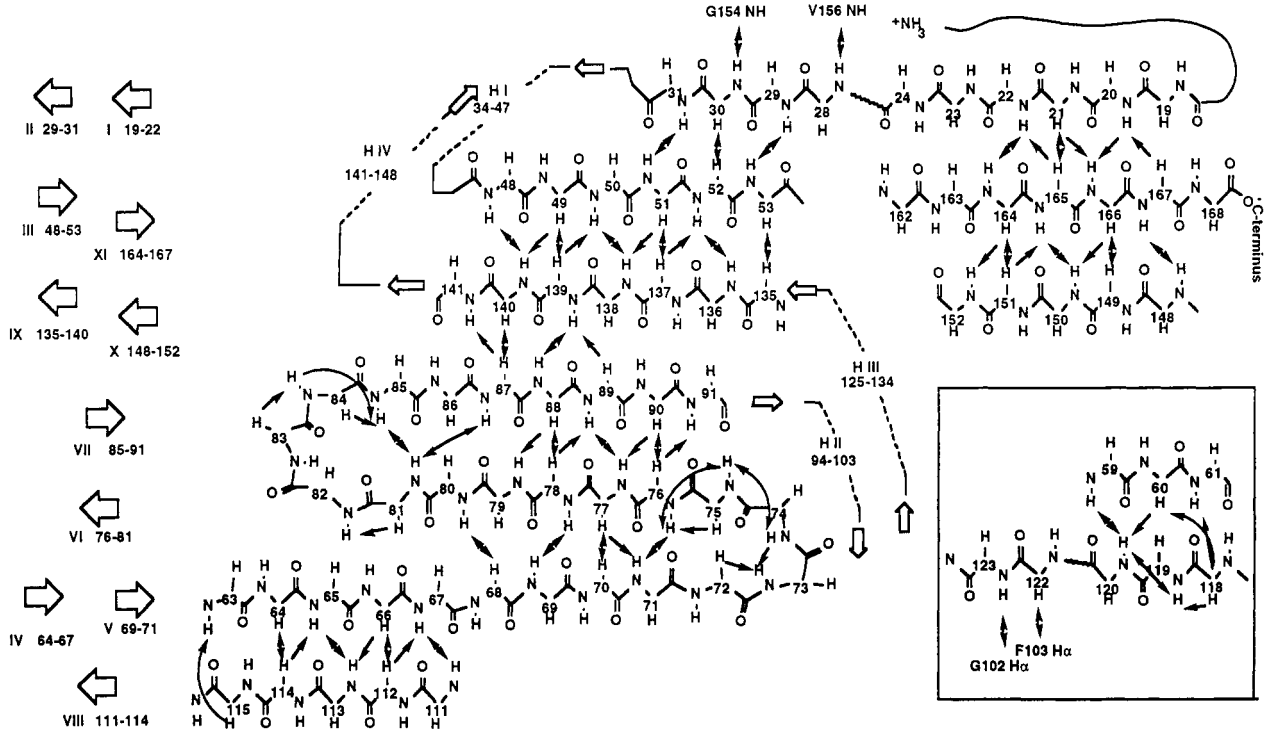

FIGURE 6: β-Sheet structure of P-III^{Glc}. White arrows denote β-strands; black arrows represent long-range NOEs observed in 3D ^{15}N and ^{13}C NOESY-HMQC spectra. Arrowheads represent observed direction of magnetization transfer. Each of the regions HI through HIV contains a helical segment of the protein together with flanking residues in coil or turn conformations.

$d_{\alpha N}$, d_{NN}, and $d_{\alpha\alpha}$ NOEs observed in spectra of P-III^{Glc} were also observed in our earlier study of III^{Glc}. Exceptions were an NOE between Lys-167 Hα (5.03 ppm) and Thr-19 Hα (4.87 ppm), which was obscured by the strong diagonal, and the missing NOE between Val-31 NH and Ile-52 Hα in spectra of P-III^{Glc}. Although the latter correlation was not observed, d_{NN}(31,51) and $d_{\alpha\alpha}$(30,52) NOEs observed in the spectrum of P-III^{Glc} confirmed the close proximity of strands βII and βIII.

Finally, we note that during our comparison of 3D ^{15}N NOESY-HMQC spectra of III^{Glc} and P-III^{Glc} we identified new NOEs in the 3D ^{15}N NOESY-HMQC spectrum of III^{Glc} between (a) Glu-43 NH and Ala-42 Hβ, (b) N32 NH and Val-31 Hα, and (c) Asn-142 NH and Ser-141 Hβ. We have also revised our previously reported estimate of the NOE cross peak intensity of Leu-87 NH–Glu-86 Hβ from medium to weak, the cross peak intensity between Ala-131 NH and Lys-130 Hα from strong to medium, the cross peak intensity between NH protons of Asp-94 and Thr-95 from strong to medium, and the cross peak intensity between Asn-142 NH and Ser-141 Hα from strong to weak (Pelton et al., 1991b). These new and revised NOE intensities for III^{Glc} do not change the conclusions with regard to the secondary structure of III^{Glc} outlined earlier (Pelton et al., 1991b). Furthermore these changes are in agreement with the NOE intensities observed from the corresponding residues in P-III^{Glc}, with the exception of the NOE between NH protons of D94 and T95 described previously (Table I).

Discussion

III^{Glc} has diverse physiological functions, one of which is to act as a phosphocarrier protein between the cytosol and the plasma membrane. In this process it accepts a phosphate group from HPr and donates it to the membrane-associated protein IIB^{Glc}. III^{Glc} also functions to regulate the uptake and catabolism of non-PTS sugars. In proposed models (Roseman & Meadow, 1990), this regulatory function depends on the phosphorylation state of III^{Glc}, which is directly correlated with the availability of glucose in the environment. III^{Glc} inhibits the activity of glycerol kinase and is thought to inhibit the lactose, melibose, maltose, and glycerol permeases, while P-III^{Glc} is thought to have no effect on these systems. In contrast, P-III^{Glc} has been proposed to stimulate adenylate cyclase (Meadow et al., 1990; Roseman & Meadow, 1990; Saier, 1989; Postma & Lengeler, 1985). Thus, phosphorylation dramatically alters the function of III^{Glc} in the cell.

The first NMR study of the phosphorylated and unphosphorylated forms of III^{Glc} from *E. coli* was reported by Dörschug et al. (1984). Upon phosphorylation, minor chemical shift changes were observed in the aromatic region of 1D ^{1}H spectra; however, it was not possible to determine if or to what extent these shifts were the result of conformational changes.

With the use of 3D heteronuclear NMR techniques (Ikura et al., 1990a, 1991; Kay et al., 1990a) combined with the availability of uniformly ^{15}N- and ^{15}N/^{13}C-labeled protein samples, we assigned nearly all of the ^{1}H, ^{15}N, and ^{13}C resonances of III^{Glc} and identified many elements of secondary structure (Pelton et al., 1991a,b). Similar studies of phospho-III^{Glc} were complicated by the short half-life for hydrolysis of P-III^{Glc} (approximately 1.5 h at pH 6.4) (Meadow & Roseman, 1982). Through the use of a regeneration system that included excess PEP and catalytic amounts of HPr and Enzyme I (Waygood et al., 1979), it was possible to keep III^{Glc} phosphorylated for several days, and, as a consequence, 3D heteronuclear techniques could be applied to the sequential assignment and structure determination of the phosphorylated protein. As stated previously (Pelton et al., 1991a), with these techniques it is possible to make sequential assignments without assumptions regarding the secondary or the tertiary structure of the protein.

The chemical shift of a nucleus is sensitive to changes in conformation and local environment. As can be seen in Figure 3, the great majority of NH, ^{15}N, Hα, ^{13}Cα signals do not shift significantly upon phosphorylation. These data indicate that

the structure of III^{Glc} does not undergo global changes due to phosphorylation of His-90. Residues whose NH, Hα, ^{15}N, and $^{13}C\alpha$ signals exhibit shifts are clustered into four groups, which are in close proximity to the active site histidines (Figures 3 and 4). Some of the largest chemical shift changes are observed for residues within the segment His-90–Leu-98 that forms a ridge very close to the side chains of His-75 and His-90. Smaller changes are observed for residues within the segments Phe-41–Val-46 and Lys-132–Leu-135 that form similar ridges further removed from the active site. The observed chemical shift changes could result either from localized conformational changes at the active site or from differences in shielding as a consequence of phosphorylation.

The close correspondence between NOE cross peak patterns in 3D ^{15}N NOESY-HMQC spectra of III^{Glc} and P-III^{Glc} for those residues whose ^{15}N–^{1}H signals exhibit large shifts (Figure 5) indicates that large conformational changes do not occur at the active site upon phosphorylation. However, small conformational changes as evidenced by changes in NOEs to the protons of Ala-76, Asp-94, and Val-96 were noted (Table I). In the X-ray structure of the unphosphorylated protein, these three residues are in close proximity to the active site histidines (Worthylake et al., 1991; Figure 4). For Ala-76, the changes are relatively small, indicating that only slight conformational changes occur upon phosphorylation (<1 Å). The similarity of NOEs between NH protons of His-75 and Ala-76 (Figures 2 and 5A) and between the Hα protons of Ala-76 and His-90 (Figure 6) in spectra of III^{Glc} and P-III^{Glc} supports this conclusion and shows that the backbone structure of Ala-76 as well as His-75 and His-90 remain intact in the phosphorylated state. Similarly, with the exception of the observed changes in NOEs to the Hγ protons of Val-96 (Table I), the equivalence of the cross peak patterns for Val-96 and Glu-97 in spectra of III^{Glc} and P-III^{Glc} (Figure 5B) shows that the backbone structure of these residues remains the same and that the conformational changes are localized to the side-chain atoms of Val-96.

Comparison of NOE cross peak patterns for Asp-94 in spectra of III^{Glc} and P-III^{Glc} revealed the most pronounced differences (Table I). Aside from a new unassigned cross peak that appears at 4.66 ppm, intensity changes in the NOEs between Asp-94 NH and both Thr-95 NH and His-90 CH^{ϵ} (Table I) were noted. These data combined with the observation that most of the NOEs to Thr-95 and His-90 do not change in intensity (Figures 2 and 5A, Table I) indicate that the NH group of Asp-94 shifts slightly (<1.5 Å) toward the CH^{ϵ} ring proton of His-90 and away from the NH proton of Thr-95. In the X-ray study of III^{Glc} (Worthylake et al., 1991), it was noted that the NH protons of Asp-94 and Thr-95 point directly toward the active site histidines, with the NH proton of Asp-94 only 4.4 Å from His-90 N^{ϵ}. The relatively small conformational changes observed for Asp-94 and Thr-95 and the other residues that comprise the active site support the suggestion of Worthylake et al. (1991) based on the X-ray structure of the unphosphorylated protein that the NH groups of Asp-94 and Thr-95 help to stabilize phospho-III^{Glc} through the interaction of these protons with the phosphate oxygens.

The strong similarity between sequential, medium, and long-range NOEs summarized in Figures 2 and 6 with those obtained for the unphosphorylated protein (Pelton et al., 1991b), supports the conclusion based on NH, ^{15}N, Hα, and $^{13}C\alpha$ chemical shift data (Figures 3 and 4) that III^{Glc} does not undergo large conformational changes upon phosphorylation. Thus, changes in structure appear to be limited to minor displacements (<1.5 Å) of residues such as Asp-94, Ala-76, and Val-96 located at the active site (Figure 4). Similar results are expected for sugar-specific proteins homologous to III^{Glc} (Meadow et al., 1990; Liao et al., 1991).

Through model building and analysis of X-ray data of a chloroplatinate heavy atom derivative of III^{Glc} from *E. coli* in which the metal was coordinated to N^{ϵ} (N3) atoms of active site residues His-75 and His-90, it was predicted that addition of a phosphoryl group would not result in large structural changes (Worthylake et al., 1991). Similar conclusions were made in regard to the IIA^{Glc} domain derived from *B. subtilis* (Liao et al., 1991). The results obtained herein on the phosphorylated form of III^{Glc} are consistent with the proposed models. Hence, the structure of III^{Glc} and proposed structures of P-III^{Glc} are appropriate when considering the interaction of this protein with other PTS and non-PTS proteins. Whether structural changes are induced in III^{Glc} upon binding to proteins such as HPr and IIB^{Glc}, however, is unknown.

In contrast to the minor structural changes observed upon phosphorylation of III^{Glc}, large structural changes have been observed upon phosphorylation of III^{Lac} from *Staphylococcus aureus*. Evidence includes changes in circular dichroism and 1D NMR spectra, antibody recognition, and polyacrylamide gel electrophoresis of phosphorylated and unphosphorylated forms of the protein (Deutscher et al., 1982). III^{Lac} differs from III^{Glc} in that it consists of three identical subunits (Hays et al., 1973; Schrecker & Hengstenberg, 1971). Each subunit can be phosphorylated, and all three phosphoryl groups are transferred to the sugar substrate (Deutscher et al., 1982; Simoni et al., 1973).

Phosphorylated and unphosphorylated forms of two proteins have also been studied by X-ray methods. For isocitrate dehydrogenase, only minor structural changes were observed upon phosphorylation of a specific serine residue, and these changes were determined to be nonessential for regulation of this enzyme (Hurley et al., 1990). However, for glycogen phosphorylase, it was found that the disordered N-terminus folded into a distorted 3_{10} helix upon phosphorylation of Ser-14 (Sprang et al., 1988). The structural changes resulted in an altered affinity for allosteric regulators. Thus, from the present data it appears that the effects of phosphorylation on protein structure can range from very minor changes as in the case of III^{Glc} and isocitrate dehydrogenase to pronounced structural rearrangements as in the case of III^{Lac} and glycogen phosphorylase. Irrespective of whether large structural changes do or do not occur, however, it is clear that phosphorylation can profoundly affect protein function.

Acknowledgments

We acknowledge Drs. A. Bax, D. Garrett, M. Ikura, L. Kay, D. Marion, and R. Powers for generously providing pulse sequences and computer software needed to process the 3D data sets, and we thank R. Tschudin and R. Rendle for expert technical support. We also thank Prof. S. J. Remington at the University of Oregon for providing X-ray derived coordinates for III^{Glc} from *E. coli* prior to publication.

Supplementary Material Available

Four figures consisting of a ^{15}N HSQC spectrum of P-III^{Glc}N and representative data from 3D HCCH-COSY and HCCH-TOCSY spectra of P-III^{Glc} and one table containing NH, ^{15}N, ^{1}H, $^{13}C\alpha$, and $^{13}C\beta$ signal assignments of P-III^{Glc} (11 pages). Ordering information is given on any current masthead page.

References

Bax, A. (1989) *Annu. Rev. Biochem. 58*, 223–256.

Bax, A., Ikura, M., Kay, L. E., Torchia, D. A., & Tschudin, R. (1990a) *J. Magn. Reson. 86*, 304–318.
Bax, A., Clore, G. M., Driscoll, P. C., Gronenborn, A. M., Ikura, M., & Kay, L. E. (1990b) *J. Magn. Reson. 87*, 620–627.
Bax, A., Clore, G. M., & Gronenborn, A. M. (1990c) *J. Magn. Reson. 88*, 425–431.
Beneski, D. A., Nakazawa, A., Weigel, N., Hartman, P. E., & Roseman, S. (1982) *J. Biol. Chem. 257*, 14492–14498.
Clore, G. M., & Gronenborn, A. M. (1991) *Science 252*, 1390–1399.
Clore, G. M., Bax, A., Driscoll, P. C., Wingfield, P. T., & Gronenborn, A. M. (1990) *Biochemistry 29*, 8172–8184.
Deutscher, J., Beyreuther, K., Sobek, H. M., Stüber, K., & Hengstenberg, W. (1982) *Biochemistry 21*, 4867–4873.
Dörschug, M., Frank, R., Kalbitzer, R. H., Hengstenberg, W., & Deutscher, J. (1984) *Eur. J. Biochem. 144*, 113–119.
El-Kabbani, O. A. L., Waygood, E. B., & Delbaere, L. T. J. (1987) *J. Biol. Chem. 262*, 12926–12929.
Fairbrother, W. J., Cavanagh, J., Dyson, H. J., Palmer, A. G., III, Sutrina, S. L., Reizer, J., Saier, M. H., Jr., & Wright, P. E. (1991) *Biochemistry 30*, 6896–6907.
Garrett, D. S., Powers, R., Gronenborn, A. M., & Clore, G. M. (1991) *J. Magn. Reson. 95*, 214–220.
Gonzy-Treboul, G., & Steinmetz, M. (1987) *J. Bacteriol. 169*, 2287–2290.
Hammen, P. K., Waygood, E. B., & Klevit, R. E. (1991) *Biochemistry 30*, 11842–11850.
Hays, J. B., Simoni, R. D., & Roseman, S. (1973) *J. Biol. Chem. 248*, 941–956.
Howarth, O. W., & Lilley, D. J. M. (1978) *Prog. Nucl. Magn. Reson. Spectrosc. 12*, 1–40.
Hurly, J. H., Dean, A. M., Sohl, J. L., Koshland, D. E., Jr., & Stroud, R. M. (1990) *Science 249*, 1012–1016.
Ikura, M., Kay, L. E., & Bax, A. (1990a) *Biochemistry 29*, 4659–4667.
Ikura, M., Kay, L. E., Tschudin, R., & Bax, A. (1990b) *J. Magn. Reson. 86*, 204–209.
Ikura, M., Kay, L. E., Krinks, M., & Bax, A. (1991) *Biochemistry 30*, 5498–5504.
Kalbitzer, H. R., Deutscher, J., Hengstenberg, W., & Rösch, P. (1981) *Biochemistry 20*, 6178–6185.
Kalbitzer, H. R., Hengstenberg, W., Rösch, P., Muss, H. P., Bernsmann, R., & Dörschug, M. (1982) *Biochemistry 21*, 2879–2885.
Kalbitzer, H. R., Muss, H. P., Engelmann, R., Kiltz, H. H., Stuber, K., & Hengstenberg, W. (1985) *Biochemistry 24*, 4562–4589.
Kalk, A., & Berendsen, H. J. C. (1976) *J. Magn. Reson. 24*, 343–366.
Kapadia, G., Reizer, J., Sutrina, S. L., Saier, M. H., Jr., Reddy, P., & Herzberg, O. (1990) *J. Mol. Biol. 211*, 1–2.
Kay, L. E., Marion, D., & Bax, A. (1989) *J. Magn. Reson. 84*, 72–84.
Kay, L. E., Ikura, M., Tschudin, R., & Bax, A. (1990a) *J. Magn. Reson. 89*, 496–514.
Kay, L. E., Ikura, M., & Bax, A. (1990b) *J. Am. Chem. Soc. 112*, 888–889.
Klevit, R. E., & Waygood, E. B. (1986) *Biochemistry 25*, 7774–7781.
Kraulis, P. (1991) *J. Appl. Crystallogr.* (in press).
Liao, D.-I., Kapadia, G., Reddy, P., Saier, M. H., Jr., Reizer, J., & Herzberg, O. (1991) *Biochemistry 30*, 9583–9594.
Live, D. H., Davis, D. G., Agosta, W. C., & Cowburn, D. (1984) *J. Am. Chem. Soc. 106*, 1939–1941.
Marion, D., Ikura, M., & Bax, A. (1989a) *J. Magn. Reson. 84*, 425–430.
Marion, D., Kay, L. E., Sparks, S. W., Torchia, D. A., & Bax, A. (1989b) *J. Am. Chem. Soc. 111*, 1515–1517.
Marion, D., Driscoll, P. C., Kay, L. E., Wingfield, P. T., Bax, A., Gronenborn, A. M., & Clore, G. M. (1989c) *Biochemistry 28*, 6150–6156.
Meadow, N. D., & Roseman, S. (1982) *J. Biol. Chem. 257*, 14526–14537.
Meadow, N. D., Coyle, P., Komoryia, A., Anfinsen, C. B., & Roseman, S. (1986) *J. Biol. Chem. 261*, 13504–13509.
Meadow, N. D., Fox, D. K., & Roseman, S. (1990) *Annu. Rev. Biochem. 59*, 497–542.
Neidhardt, F. C., Block, P. L., & Smith, D. F. (1974) *J. Bacteriol. 119*, 736–747.
Pelton, J. G., Torchia, D. A., Meadow, N. D., Wong, C.-Y., & Roseman, S. (1991a) *Biochemistry 30*, 10043–10057.
Pelton, J. G., Torchia, D. A., Meadow, N. D., Wong, C.-Y., & Roseman, S. (1991b) *Proc. Natl. Acad. Sci. U.S.A. 88*, 3479–3488.
Postma, P. W., & Lengeler, J. (1985) *Microbiol. Rev. 49*, 232–269.
Presper, K. A., Wong, C.-Y., Liu, L., Meadow, N. D., & Roseman, S. (1989) *Proc. Natl. Acad. Sci. U.S.A. 86*, 4052–4055.
Roseman, S., & Meadow, N. D. (1990) *J. Biol. Chem. 265*, 2993–2996.
Saier, M. H., Jr. (1989) *Microbiol. Rev. 53*, 109–120.
Schrecker, O., & Hengstenberg, W. (1971) *FEBS Lett. 13*, 209–212.
Shaka, A. J., Lee, C. J., & Pines, A. (1988) *J. Magn. Reson. 77*, 274–293.
Simoni, R. D., Hays, J. B., Nakazawa, T., & Roseman, S. (1973) *J. Biol. Chem. 248*, 957–965.
Spera, S., & Bax, A. (1991) *J. Am. Chem. Soc. 113*, 5490–5492.
Sprang, S. R., Acharya, K. R., Goldsmith, E. J., Stuart, D. I., Varvill, K., Fletterick, R. J., Madsen, N. B., & Johnson, L. N. (1988) *Nature 336*, 215–221.
Studier, F. W., & Moffatt, B. A. (1986) *J. Mol. Biol. 189*, 113–130.
Waygood, E. B., Meadow, N. D., & Roseman, S. (1979) *Anal. Biochem. 95*, 293–304.
Weigel, N., Waygood, E. B., Kukuruzinska, M. A., Nakazawa, A., & Roseman, S. (1982) *J. Biol. Chem. 257*, 14461–14469.
Wishart, D. S., Sykes, B. D., & Richards, F. M. (1991) *J. Mol. Biol. 222*, 311–333.
Witanowski, M., Stefaniak, L., & Webb, G. A. (1986) *Annu. Rep. NMR Spectrosc. 18*, 4–763.
Wittekind, M., Reizer, J., Deutscher, J., Saier, M. H., Jr., & Klevit, R. E. (1989) *Biochemistry 28*, 9908–9912.
Wittekind, M., Reizer, J., & Klevit, R. E. (1990) *Biochemistry 29*, 7191–7200.
Worthylake, D., Meadow, N. D., Roseman, S., Liao, D.-I., Herzberg, O., & Remington, S. J. (1991) *Proc. Natl. Acad. Sci. U.S.A. 88*, 10382–10386.
Wüthrich, K. (1986) *NMR of Proteins and Nucleic Acids*, Wiley, New York.